

## Seismic Motion Incoherency Effects for AP1000 Nuclear Island Complex

Dan M. Ghiocel<sup>a</sup>, Dali Li<sup>b</sup>, Keith Coogler<sup>b</sup>, and Leonardo Tunon-Sanjur<sup>b</sup>

<sup>a</sup>*Ghiocel Predictive Technologies, Inc., 6 South Main St., Pittsford, New York 14534, USA,  
E-mail: dan.ghiocel@ghiocel-tech.com*

<sup>b</sup>*Westinghouse, 1000 Westinghouse Drive, Cranberry Township, Pennsylvania 16066, USA*

**Keywords:** soil-structure interaction, motion incoherency, incoherent, rock site, nuclear island, seismic.

### 1 ABSTRACT

The paper addresses the seismic motion incoherency effects on the soil-structure interaction (SSI) response of the AP1000 nuclear complex. The paper addresses both theoretical and practical aspects of seismic incoherent SSI analysis. The paper describes briefly the theoretical basis and specific implementation aspects related to the stochastic and deterministic incoherent SSI approaches. These incoherent SSI approaches were benchmarked by Electric Power Research Institute (EPRI). Two different structural models of AP1000 NI complex are considered: i) the AP1000-based stick model (used in the EPRI studies) and ii) AP1000 NI20 finite element model (used by Westinghouse for computation of in-structure response spectra). The AP1000 NI20 model was assumed for sensitivity studies with both flexible and rigid basemat. Using AP1000-based stick model, comparative results are shown for a hard-rock site and a soft soil site. Hard-rock high frequency and Regularity Guide 1.60 ground spectra were considered for the two site soil conditions. The recent Abrahamson plane-wave coherency models for hard-rock and soil conditions were applied. The effect of foundation flexibility on the coherent and incoherent SSI responses is discussed using the AP1000 NI20 model with flexible-basemat and rigid-basemat, respectively. Finally, few incoherent SSI analysis recommendations are stated.

### 2 SEISMIC MOTION INCOHERENCY

Seismic motion incoherency is produced by the local random spatial variation of ground motion in horizontal plane in the vicinity of building foundations. To capture the spatial variability of the ground motion in horizontal plane, a stochastic field model is required. Assuming that the spatial variation of the ground motion at different locations could be defined by a homogeneous and isotropic Gaussian stochastic field, its spatial variability is completely defined by its coherency spectrum, or coherence function. Due to the isotropy assumption, the coherence functions defined for any arbitrary direction are the same function called isotropic coherence function. This isotropic coherence function is one-dimensional function with respect to the relative distance between locations, i.e. directional orientation of locations in horizontal plane is not considered.

For a seismic wave stochastic field, with an amplitude denoted  $u(t)$  in time domain and  $U(\omega)$  in frequency domain, the (pair) cross-spectral density (CSD) function for two separated locations on ground surface  $j$  and  $k$ ,  $S_{U_j, U_k}(\omega)$ , is expressed by

$$S_{U_j, U_k}(\omega) = [S_{U_j, U_j}(\omega)S_{U_k, U_k}(\omega)]^{1/2} \Gamma_{U_j, U_k}(\omega) \quad (1)$$

where  $S_{U_j, U_j}(\omega)$  and  $S_{U_k, U_k}(\omega)$  are the power spectral density (PSD) of the seismic motion at locations  $j$  and  $k$ , and  $\Gamma_{U_j, U_k}(\omega)$  is the pair coherence function for locations  $j$  and  $k$ . The coherence function,  $\Gamma_{U_j, U_k}(\omega)$  is a similarity measurement of the two location motions including both the amplitude spatial variation and the wave passage effects.

More generally, the CSD function and coherence function are complex quantities. The complex coherent function is called the “unlagged” coherence function (Abrahamson, 2007). However, in engineering practice, the “lagged” coherence functions that is a real and positive quantity defined by the amplitude of the

complex coherence function is used instead of the “unlagged” complex coherence function. Further, if the horizontal apparent wave velocity is considered a constant for all frequencies, then, the “plane-wave” coherency model is defined. The plane-wave coherency models, such those provided by Abrahamson (2007), are used in practice in conjunction with the seismic plane-wave propagation SSI codes.

From Equation 1, it should be noted that the coherence function at any given frequency is identical with the statistical correlation coefficient, sometime also called scaled covariance function, between the two random variables defined in frequency domain by the amplitudes of ground motion at two locations. This observation suggests that a series of efficient engineering numerical tools developed for digital simulation of stochastic spatial variation fields based on factorization of covariance kernels could be extended for simulation of seismic motion incoherency using factorization of coherence kernels at each frequency.

Currently, based on significant seismological database information recorded in many dense arrays, Abrahamson (2007) defined a set of specific coherency functions for different soil conditions and foundation type for 1) all site conditions and shallow foundations, 2) all site conditions and embedded foundations, 3) for hard-rock sites and shallow and embedded foundations, and 4) soil sites and shallow foundations.

### 3 INCOHERENT SSI METHODOLOGY

In this section, the seismic incoherent SSI analysis methodologies used in the recent EPRI studies (Short, Hardy, Mertz and Johnson, 2006, 2007) that were implemented in the ACS SASSI code (Ghiocel, 2009) are described. These methodologies are based on the spectral factorization model proposed by Tseng and Lilhanand (1997). The basic equations shown in this section are described using same notations with Tseng and Lilhanand. The main differences in notation are that for structural degree-of-freedom (dof), we used superscript s instead of subscript s, and for ground motion at interaction nodes we used superscript g instead of subscript g.

#### 3.1 Incoherent Free-Field Motion Calculations

The coherent free-field motion at any interaction node dof k,  $U_k^{g,c}(\omega)$  is computed by:

$$U_k^{g,c}(\omega) = H_k^{g,c}(\omega)U_0^g(\omega) \quad (2)$$

where  $H_k^{g,c}(\omega)$  is the (deterministic) complex coherent ground transfer function vector at interface nodes and  $U_0^g(\omega)$  is the complex Fourier transform of the control motion. Similarly, the incoherent free-field motion at any interaction node dof k,  $U_k^{g,i}(\omega)$  is computed by:

$$U_k^{g,i}(\omega) = \tilde{H}_k^{g,i}(\omega)U_0^g(\omega) \quad (3)$$

where  $\tilde{H}_k^{g,i}(\omega)$  is the (stochastic) incoherent ground transfer function vector at interaction node dofs and  $U_0^g(\omega)$  is the complex Fourier transform of the control motion. The main difference between coherent and incoherent free-field transfer function vectors is that the  $H_k^{g,c}(\omega)$  is deterministic quantity while  $\tilde{H}_k^{g,i}(\omega)$  is a stochastic quantity (the tilda represents a stochastic quantity) that includes deterministic effects due to the seismic plane-wave propagation, but also stochastic effects due to incoherent motion spatial variation in horizontal plane. Thus, the incoherent free-field transfer function at any interaction node can be defined by:

$$\tilde{H}_k^{g,i}(\omega) = S_k(\omega)H_k^{g,c}(\omega) \quad (4)$$

where  $S_k(\omega)$  is a frequency-dependent quantity that includes the effects of the stochastic spatial variation of free-field motion at any interaction node dof k due to incoherency. In fact, in the numerical implementation based on the complex frequency approach,  $S_k(\omega)$  represents the complex Fourier transform of relative spatial random variation of the motion amplitude at the interaction node dof k due to incoherency. Since these relative spatial variations are random,  $S_k(\omega)$  is stochastic in nature. The stochastic  $S_k(\omega)$  can be computed for each interaction node dof k using spectral factorization of coherency matrix computed for all SSI interaction nodes. For any interaction node dof k, the stochastic spatial motion variability transfer

function  $\tilde{H}_k^{g,i}(\omega)$  in complex frequency domain is described by the product of the stochastic eigen-series expansion of the spatial incoherent field times the deterministic complex coherent ground motion transfer function:

$$\tilde{H}_k^{g,i}(\omega) = \left[ \sum_{j=1}^M \Phi_{j,k}(\omega) \lambda_j(\omega) \eta_{\theta_j}(\omega) \right] H_k^{g,c}(\omega) \quad (5)$$

where  $\lambda_j(\omega)$  and  $\Phi_{j,k}(\omega)$  are the  $j$ -th eigenvalue and the  $j$ -th eigenvector component at interaction node  $k$ . The factor  $\eta_{\theta_j}(\omega)$  in Equation 5 is the random phase component associated with the  $j$ -th eigenvector that is given by  $\eta_{\theta_j}(\omega) = \exp(i\theta_j)$  in which the random phase angles are assumed to be uniformly distributed over the unit circle. The number of coherency matrix eigenvectors, or incoherent spatial modes, could be either all modes or a reduced number of modes  $M$  depending on the eigen-series convergence.

### 3.2 Incoherent SSI Response Calculations

For a coherent motion input, assuming a number of interaction nodes equal to  $N$ , the complex Fourier SSI response at any structural dof  $i$ ,  $U_i^{s,c}(\omega)$ , is computed by the superposition of the effects produced by the application of the coherent motion input at each interaction node  $k$ :

$$U_i^{s,c}(\omega) = \sum_{k=1}^N H_{i,k}^s(\omega) U_k^{g,c}(\omega) = \sum_{k=1}^N H_{i,k}^s(\omega) H_k^{g,c}(\omega) U_0^g(\omega) \quad (6)$$

where the  $H^s(\omega)$  matrix is the structural complex transfer function matrix given unit inputs at interaction node dofs. The component  $H_{i,k}^s(\omega)$  denotes the complex transfer function for the  $i$ -th structural dof if a unit amplitude motion at the  $k$ -th interaction node dof is applied. For incoherent motion input, the complex Fourier SSI response at any structural dof  $i$ ,  $U_i^{s,i}(\omega)$ , is computed similarly by the superposition of the effects produced by the application of the incoherent motion input at each interaction node  $k$ :

$$U_i^{s,i}(\omega) = \sum_{k=1}^N H_{i,k}^s(\omega) U_k^{g,i}(\omega) = \sum_{k=1}^N H_{i,k}^s(\omega) \left[ \sum_{j=1}^M \Phi_{j,k}(\omega) \lambda_j(\omega) \eta_{\theta_j}(\omega) \right] H_k^{g,c}(\omega) U_0^g(\omega) \quad (7)$$

Two types of incoherent seismic SSI analysis approaches could be used for solving Equation 7: the stochastic approach and deterministic approach. These approaches were investigated for EPRI by Short, Hardy, Merz and Johnson (2007). *Stochastic approach* is based simulating random incoherent motion realizations (Simulation Mean in EPRI studies). Using stochastic simulation algorithms, a set of random incoherent motion samples is generated at each foundation SSI interaction nodes. For each incoherent motion random sample an incoherent SSI analysis is performed. The final mean SSI response is obtained by statistical averaging of SSI response random samples. *Deterministic approach* approximates the mean incoherent SSI response using simple superposition rules of random incoherency mode effects, such as the algebraic sum (AS) (AS in EPRI studies) and the square-root of the sum of square (SRSS) (SRSS in EPRI studies).

It should be noted that for the stochastic simulation approach and the deterministic approach based on linear superposition, the number of extracted coherency matrix eigenvectors, or incoherent spatial modes, can be as large as desired with zero impact on the incoherent SSI analysis run time. By default, all the incoherent spatial modes are included. Consideration of all incoherent spatial modes improves the incoherent SSI accuracy and produces an accurate recovery of the free-field coherency matrix at the interaction nodes; this can be checked for each calculation frequency. The AS approach is fast, much faster than the stochastic approach, and it is easy to use. The SRSS approach is more difficult to apply since has no convergence criteria for the required number of incoherent spatial modes to be considered. It can be applied by a trial-and-error basis. It should also be noted that the SRSS approach requires one SSI analysis for each incoherent mode, that means that is at least several times slower than the AS approach that requires only a single SSI analysis.

In AP1000 SSI studies, we considered both stochastic and deterministic incoherent SSI approaches using ACS SASSI code (Ghiocel, 2009). In addition to stochastic simulation approach, three deterministic

approaches were considered: i) linear superposition, or algebraic sum, of the scaled incoherent spatial modes (AS in EPRI studies), ii) quadratic superposition of the incoherent modal SSI complex response amplitudes (transfer function amplitudes) assuming a zero-phase for the incoherent SSI complex response phase (SRSS in EPRI studies), and iii) quadratic superposition of the incoherent modal SSI complex response amplitudes (transfer function amplitudes) assuming a non-zero phase for the incoherent SSI complex response that is equal to coherent SSI complex response phase (not used in EPRI studies). The last implementation is an alternate version of SRSS approach that does not neglect the complex response phase.

For *rigid foundations* the incoherency-induced stochasticity of the basemat motion is driven by the global or rigid body spatial variations (integral variations) of free-field motion and, therefore, is less complex and random than free-field motion. The rigid foundation motion has a smoothed spatial variation pattern since the kinematic SSI interaction is large. Thus, the differential free-field motions are highly constrained by the rigid basemat, and because of this (rigid body), the foundation motion complexity is highly reduced in comparison with the complexity of the local motion spatial variations. For *flexible foundations*, the incoherency-induced stochasticity of the basemat motion is driven by the local spatial variations of free-field motion. The flexible foundation motion has a less smoothed spatial variation pattern since kinematic SSI is reduced. Thus, the differential free-field motions are less constrained by the basemat, and because of this, the (flexible) foundation motion complexity is similar to the complexity of the local motion spatial variations.

Based on our investigations, we noticed that due to their stochastic modeling simplicity, deterministic SSI approaches are limited to rigid foundation applications, as shown in EPRI studies (Short, Hardy, Mertz and Johnson, 2006, 2007). For flexible foundations, the stochastic simulation approach is the only choice since it accurately captures the statistical nature of the local free-field motion spatial variations. For flexible foundations, the free-field motion local spatial variations are directly transmitted to the flexible basemat motion. Deterministic approaches are not capable of capturing the local phasing of the interaction motions.

#### 4 AP1000 NUCLEAR ISLAND SSI STUDIES

For the AP1000 NI incoherent SSI analysis studies, two types of SSI models were employed: i) the AP1000-based stick model with rigid basemat (Figure 1) used in the EPRI studies, and ii) the AP1000 NI20 finite element model (Figure 2) used by Westinghouse for In Structure Response Spectra (ISRS) computation.

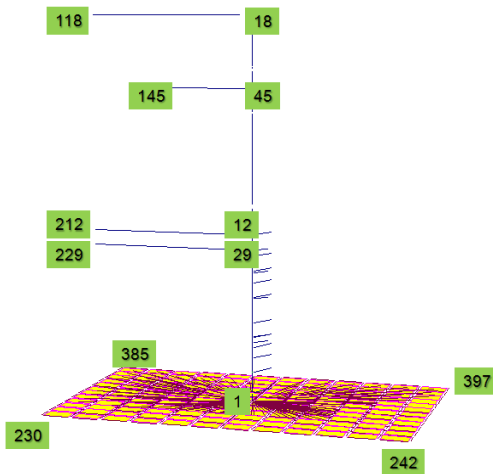


Figure 1 EPRI AP1000-Based Stick Model

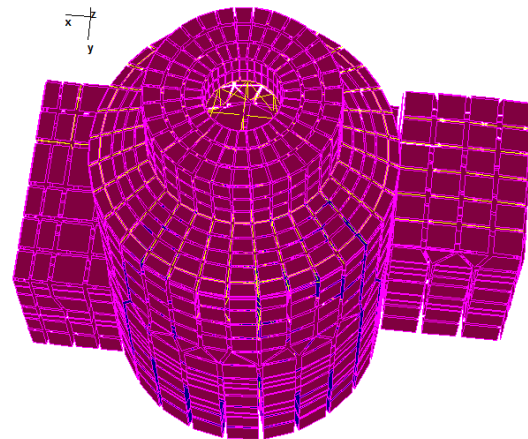


Figure 2 AP1000 NI20 Model

The AP1000 NI20 model was assumed with both flexible basemat (6ft thickness) and rigid basemat (elastic modulus amplified 10,000 times). No embedment was considered. The stochastic simulation approach was applied.

Two different site conditions were considered: i) a hard-rock site (average  $V_s$  about 8000fps) and soft soil site (average  $V_s$  about 1000fps). The seismic input was defined by a high frequency response spectra (HRHF) for the hard-rock site condition and the Regulatory Guide (RG) 1.60 spectrum for the soil site, respectively. The 2007 Abrahamson coherency models for hard-rock and soil were applied (incoherency models # 5 and 6 in ACS SASSI). However, it should be noted that the soil coherence function is not accepted by US NRC at this time. Only the hard-rock coherence function is permitted by US NRC.

The SSI response is considered in terms of the 5% damping in-structure response spectra (ISRS) computed at the basemat level and at some higher elevation levels. The combined ISRS for three-directional seismic inputs were obtained using the SRSS superposition rule of co-directional effects.

#### 4.1 AP1000-Based Stick Model

In this study, the AP1000-based stick model used in EPRI studies was further modified to reflect the horizontal foundation size of the AP1000 NI. Thus, the AP1000-based stick foundation size that was modified from 150ft x 150ft size as used in the EPRI investigation to the actual 158ft x 254ft size.

#### 4.2 AP1000 NI20 Model with Flexible and Rigid Basemats

The intention of using the rigid-base assumption was to bring “closer” the AP1000 NI20 model to the AP1000-based stick model, namely, to define both models with rigid basemats for SSI response comparisons. Also, by comparing the SSI results obtained for the AP1000 NI20 model with flexible and rigid basemat, the effects of the basemat flexibility on SSI response could be evaluated.

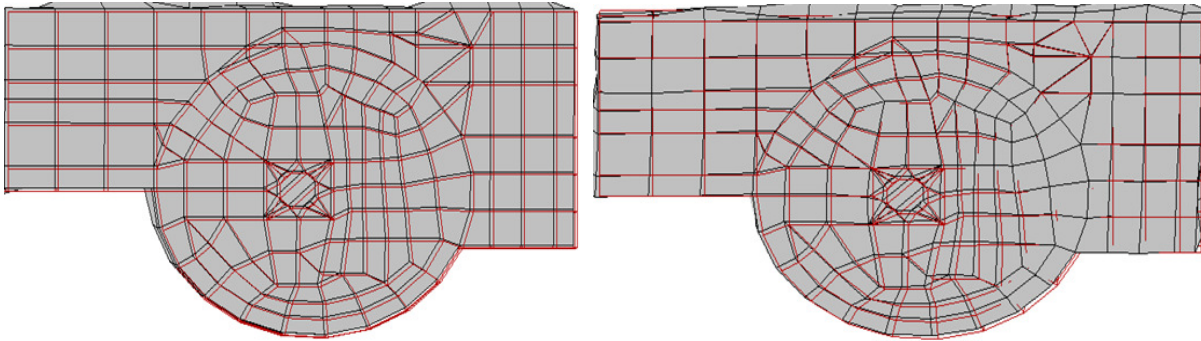


Figure 3 Coherent SSI Basemat Motion Amplitude Figure 4 Incoherent SSI Basemat Motion Amplitude

Figures 3 and 4 show the foundation motion for the AP1000 NI20 model with flexible basemat (bottom view is from underneath basemat) at an arbitrary time for three-directional seismic inputs defined by vertically propagating coherent and incoherent seismic shear and compression waves. It should be noted that while for coherent input, the foundation motion is similar to a rigid body motion in translation, since no kinematic SSI occurs, for incoherent input, the foundation motion is more complex, similar to an elastic body motion that deforms under incoherent input due to significant kinematic SSI effects.

#### 4.3 Comparative Coherent and Incoherent SSI Analysis Results

Figure 5 and 6 shows the computed incoherent and coherent ISRS in X and Z directions at the basemat center location of the AP1000-based stick model (node 1) for the rock site and the soil site, respectively. As shown, the effect of motion incoherency is significant for both the rock site (with hard-rock input and Abrahamson hard-rock coherency function), but also for soil site (with RG 1.60 input and Abrahamson soil coherency function). The ISRS reductions due to incoherency are larger for the hard-rock site, about twice than for the soil site. In high frequency range, the ISRS reductions can correspond to a knocking down factor of 3.

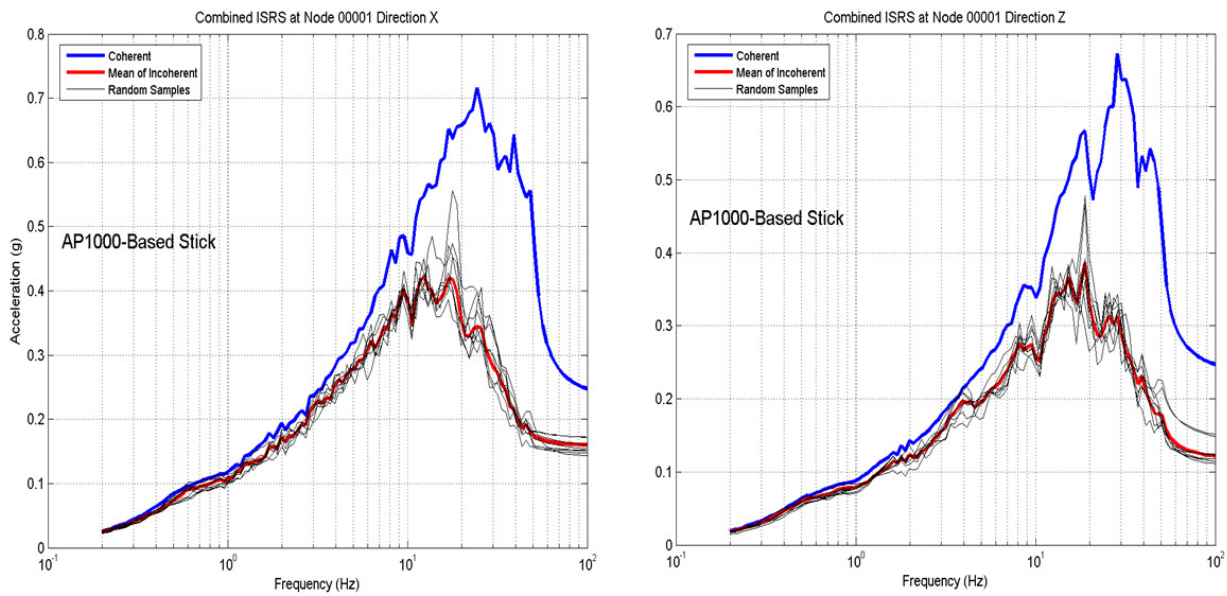


Figure 5 AP1000-based Stick Model: Incoherent and Coherent ISRS at the Basemat Center (Node 1) for Hard-Rock Site

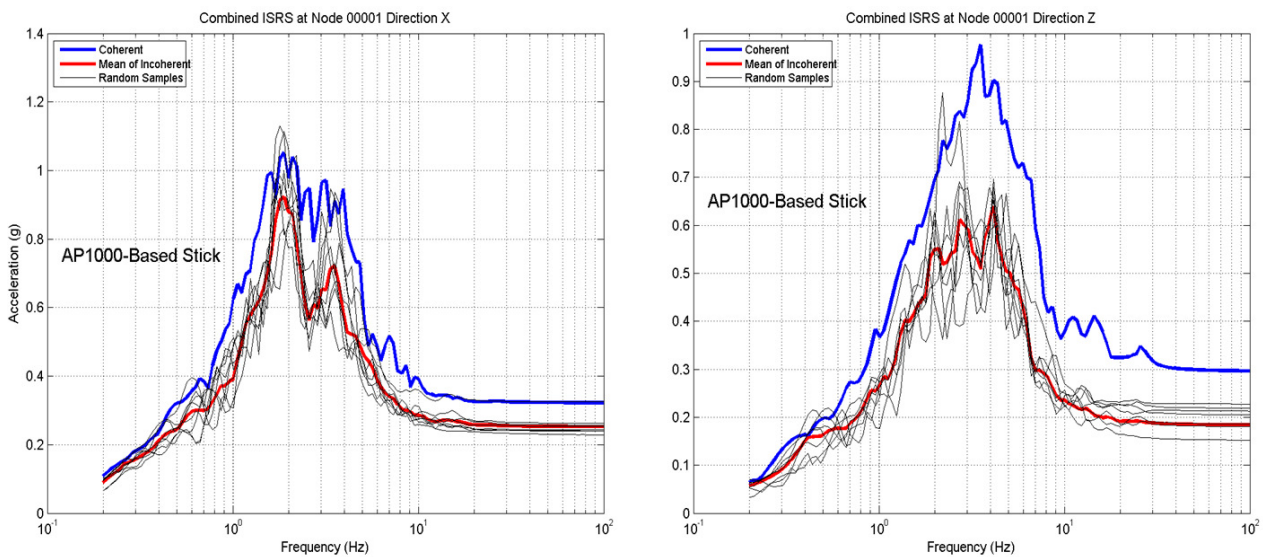


Figure 6 AP1000-based Stick Model: Incoherent and Coherent ISRS at the Basemat Center (Node 1) for Soil Site

Figures 7 and 8 show the computed incoherent and coherent ISRS in X and Z directions at the top of the containment internal structure (CIS) of the AP1000-based stick model (node 29) for the rock site and the soil site, respectively. It should be noted that the remarks made for the incoherent ISRS computed at basemat level based on Figures 5 and 6 are valid at higher elevations as shown in Figures 7 and 8. An aspect of interest from all Figures 5 through 8 is that the incoherent ISRS statistical variations (shown by the random scatter) are larger for the soil site than for the hard-rock site. This is an aspect that is currently under further consideration.

Figures 9 and 10 show the effects of the AP1000 NI20 model basemat flexibility on the computed ISRS at a higher elevation level. It appears that the basemat flexibility effect is less significant on ISRS responses. However, the basemat flexibility may amplify some structural forces for incoherent inputs when compared with those for coherent inputs due the amplified kinematic SSI effects under incoherent waves.

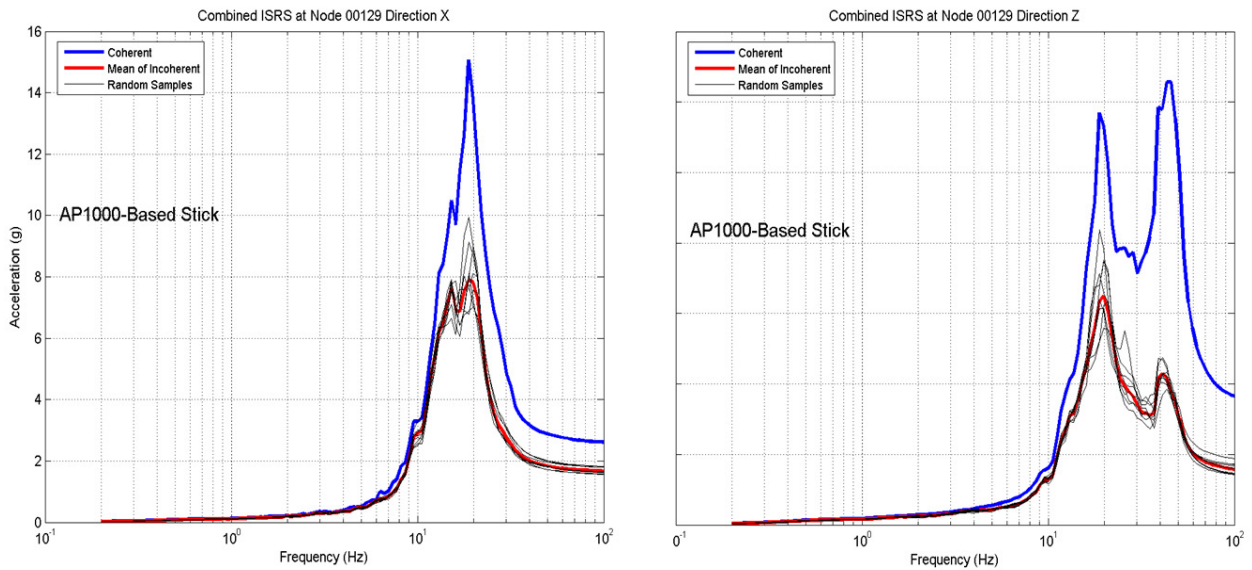


Figure 7 AP1000-based Stick Results: Incoherent and Coherent ISRS at the Top of CIS (Node 29) for Hard-Rock Site

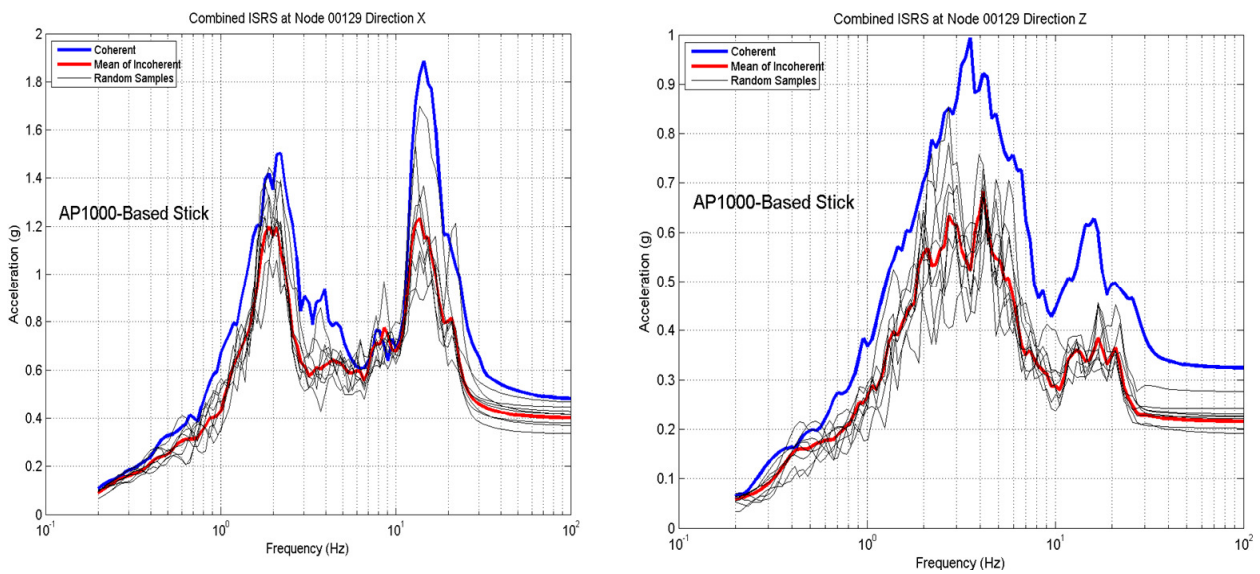


Figure 8 AP1000-based Stick Model Results: Incoherent and Coherent ISRS at the Top of CIS (Node 29) for Soil Site

## 5 CONCLUSIONS

Based on the AP1000 NI seismic SSI studies done so far, we state two important conclusions:

- 1) The effects of motion incoherency on the computed ISRS are significant for both the rock and the soil sites. The ISRS amplitude reductions were twice larger for rock sites than for soil sites, as shown herein. We believe that more study is worthwhile to propose and gain acceptance for the use of soil coherence function by the US NRC.
- 2) The basemat flexibility reduces the kinematic SSI under incoherent waves, and by this slightly decreases the motion incoherency effects on the computed ISRS.

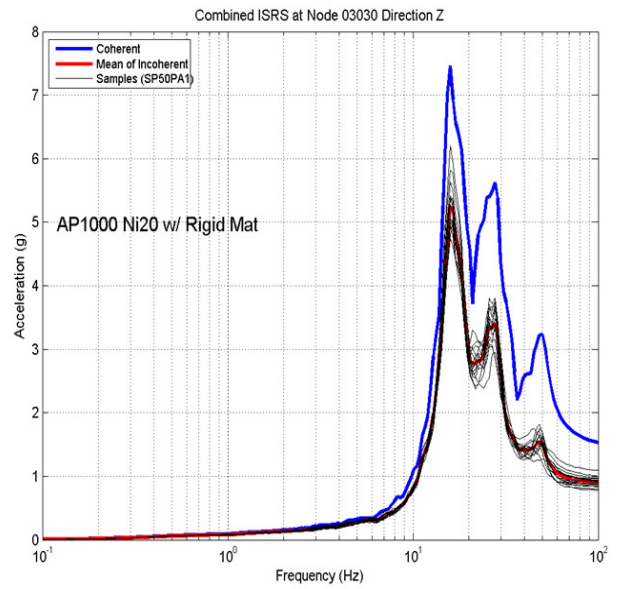
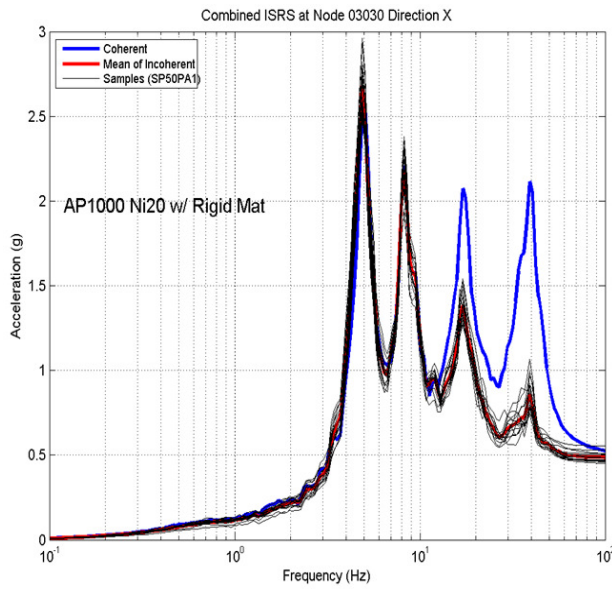


Figure 9 AP1000 NI20 with Rigid Basemat: Incoherent and Coherent ISRS at A Higher Elevation

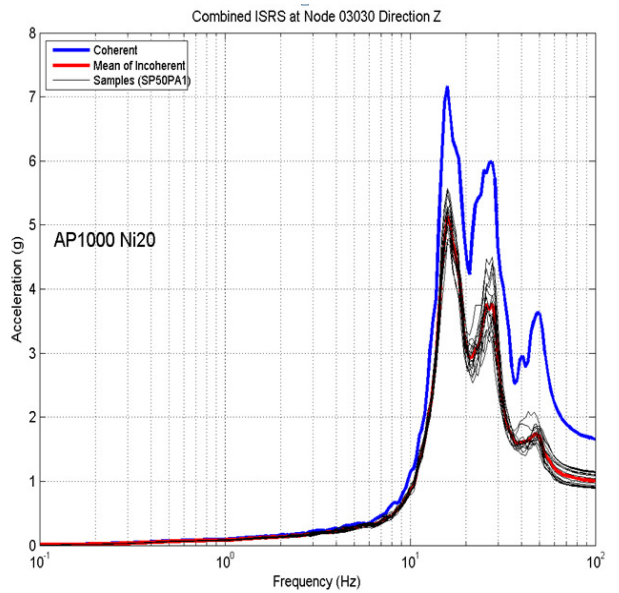
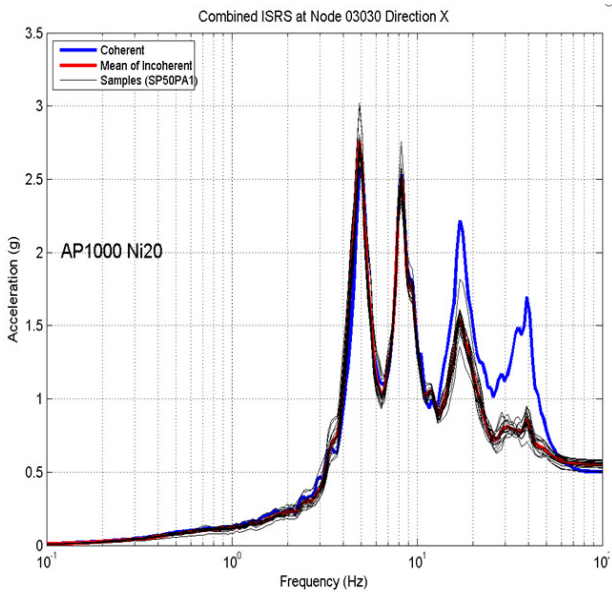


Figure 10 AP1000 NI20 with Flexible Basemat: Incoherent and Coherent ISRS at A Higher Elevation

## REFERENCES

Abrahamson, N. 2007. Effects of Seismic Motion Incoherency Effects EPRI Palo Alto, CA, TR-1015111

Ghiocel, D.M. 2009. ACS SASSI NQA Version 2.3.0, User Manuals.

Short, S.A., G.S. Hardy, K.L. Merz, and J.J. Johnson. 2007. Validation of CLASSI and SASSI to Treat Seismic Wave Incoherence in SSI Analysis of NPP Structures, EPRI Palo Alto, CA, TR-1015110

Tseng and Lilhanand.1997. Soil-Structure Interaction Analysis Incorporating Spatial Incoherence of Ground Motions, Electric Power Research Institute, Palo Alto, CA, Report No. TR-102631 2225.